Role of Electrostatics and Salt Bridges in Stabilizing the Compound I Radical in Ascorbate Peroxidase†

Tiffany P. Barrows‡ and Thomas L. Poulos*,‡,§

Departments of Molecular Biology and Biochemistry, Physiology and Biophysics, and Chemistry and Center in Chemical and Structural Biology, University of California, Irvine, California 92697

Received April 18, 2005; Revised Manuscript Received June 24, 2005

ABSTRACT: Cytochrome *c* (CcP) and ascorbate peroxidase (APX) are heme peroxidases which have very similar active site structures yet differ substantially in the properties of compound I, the intermediate formed upon reaction with peroxides. Although both peroxidases have a tryptophan in the proximal heme pocket, Trp191 in CcP and Trp179 in APX, only Trp191 in CcP forms a stable cation radical while APX forms the more traditional porphyrin π-cation radical. Previous work [Barrows, T. P., et al. (2004) *Biochemistry 43*, 8826−8834] has shown that converting three methionine residues in the cytochrome *c* peroxidase (CcP) proximal heme pocket to the corresponding residues in APX dramatically decreased the stability of the Trp191 radical in CcP compound I. On the basis of these results, we reasoned that replacing the analogous residues at positions 160, 203, and 204 in APX with methionine should stabilize a Trp179 radical in APX compound I. Steady- and transient-state kinetics of this mutant (designated APX3M) show a significant destabilization of the native porphyrin π-radical, while electron paramagnetic resonance (EPR) studies show an increase in the intensity of the signal at $g = 2.006$ with characteristics consistent with formation of a Trp radical. This hypothesis was tested by replacing Trp179 with Phe in the APX3M background. The EPR spectrum of this mutant was very similar to that of the CcP W191G mutant which is known to form a tyrosine radical. Previously published theoretical studies [Guallar, V., et al. (2003) *Proc. Natl. Acad. Sci. U.S.A. 100*, 6998−7002] suggest that electrostatic shielding of the heme propionates also plays a role in the stability of the porphyrin radical. Arg172 in APX hydrogen bonds with one of the heme propionates. Replacing Arg172 with an asparagine residue in the APX3M background generates a mutant which no longer forms the full complement of the compound I porphyrin π-radical. These results suggest that the electrostatics of the proximal pocket and the shielding of propionate groups by salt bridges are critical factors controlling the location of a stable compound I radical in heme peroxidases.

Heme peroxidases use the same overall reaction mechanism to catalyze the peroxide-dependent oxidation of a wide variety of substrates to give two oxidized substrate molecules and two molecules of water.

$$Fe^{3+}R + H_2O_2 \rightarrow \underset{\text{compound I}}{Fe^{4+}{=}OR^{\bullet+}} + H_2O \quad (1)$$

$$Fe^{4+}{=}OR^{\bullet+} + \text{substrate} \rightarrow \underset{\text{compound II}}{Fe^{4+}{=}O} + \text{oxidized substrate} \quad (2)$$

$$Fe^{4+}{=}O + \text{substrate} \rightarrow \underset{\text{resting-state enzyme}}{Fe^{3+}R} + \text{oxidized substrate} + H_2O \quad (3)$$

Despite the similar reaction cycle shared by most heme peroxidases, there are important differences between members of the superfamily of plant, fungal, and bacterial heme peroxidases. Most notable are differences in the reaction cycle of the best-characterized member of the enzyme family, cytochrome *c* peroxidase (CcP).[1] In all currently characterized heme peroxidases, with the exception of CcP, the radical in compound I ($R^{\bullet+}$ in eq 1) forms on the porphyrin. However, in compound I of CcP, experimental (*1*) and computational methods (*2*) show that the radical is stably located as a cation on Trp191 which is situated just below the heme, adjacent to the His ligand in the proximal heme pocket.

Initially, this difference was attributed to the substitution of a Phe residue in place of CcP's proximal Trp (Figure 1). Since Trp is more readily oxidized than Phe, the radical in CcP initially forms on the porphyrin but then rapidly migrates to Trp191. Studies on ascorbate peroxidase (APX), however, clearly illustrated that this simple picture is inadequate (*3*−*8*). Patterson et al. showed that in addition to a general similarity in overall structure (rmsd of 200 common Cα atoms of 1.01 Å), the proximal Trp residue was not only

† This work was funded by NIH Predoctoral Training Grant GM 07311-27 to T.P.B. and by NIH Grant GM42614.

* To whom correspondence should be addressed. E-mail: poulos@uci.edu. Fax: (949) 824-7020.

‡ Departments of Molecular Biology and Biochemistry and Center in Chemical and Structural Biology.

§ Departments of Physiology and Biophysics and of Chemistry.

[1] Abbreviations: APX, ascorbate peroxidase; APX1M, APX3M, APX3M/W179F, and APX3M/R172N, mutants of APX; CcP, cytochrome *c* peroxidase; EPR, electron paramagnetic resonance; IPTG, isopropyl β-D-thiogalactopyranoside.

10.1021/bi0507128 CCC: $30.25
Published on Web 10/04/2005

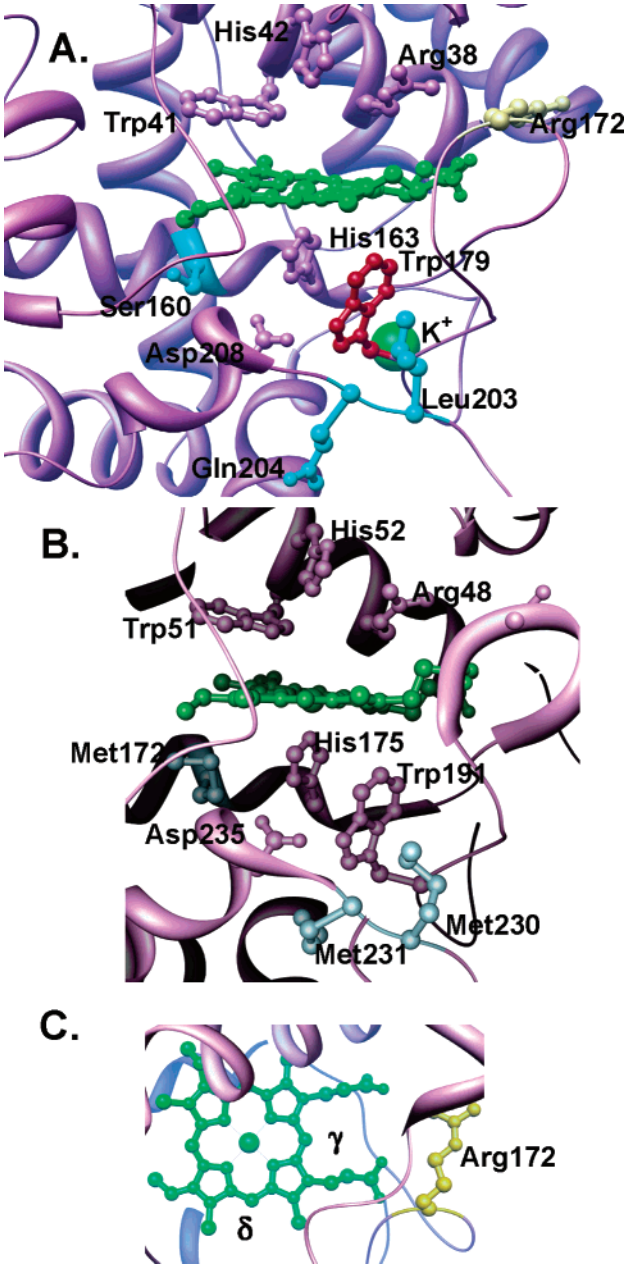

FIGURE 1: Comparison of APX (A) and CcP (B) active sites. The active sites of the two enzymes both contain the proximal hydrogen-bonded triad (His-Asp-Trp). The heme group of APX represented in panel C shows the location of the two substrate binding sites in APX. The structures were created and rendered using Chimera (*32*). The structure representing APX can be accessed as Protein Data Bank entry 1APX (*5*, *33*).

present in APX but also locked in the same hydrogen-bonded triad, His-Asp-Trp, as in CcP (*5*). Quite unexpectedly, however, EPR studies showed that the radical species in compound I of APX is the more common porphyrin π-cation radical, rather than the Trp cation radical that occurs in compound I of CcP (*6*). Further work by Pappa et al. (*4*) showed that the proximal Trp residue, essential to activity in CcP, could be replaced with a Phe in APX with no effect on the rates of compound I formation or steady-state substrate oxidation (*4*).

These observations led us to a series of studies in an attempt to understand why CcP forms a stable Trp191 radical while APX does not. This work focused primarily on enhanced electrostatic stabilization of the Trp cation radical in CcP (*9*−*13*). APX contains a K^+ ion located ~8 Å from Trp179, while CcP has only a water molecule at this position. It was reasoned that the additional positive charge in APX would destabilize the positive charge on the Trp cation radical, thus favoring the porphyrin π-cation radical in APX. To test this hypothesis, Bonagura et al. (*9*, *10*) engineered the K^+ site into CcP, and indeed, the Trp191 radical was found to be much less stable. Barrows et al. (*13*) then showed that a full oxidizing equivalent can still form on Trp191 in the CcP mutant containing the K^+ site but that it rapidly migrates to other sites in CcP, most likely, Tyr residues. These results indicated that other factors besides the absence of K^+ in CcP help to stabilize the Trp191 radical. We also showed that these other factors include three Met residues unique to the proximal pocket of CcP whose electron-rich sulfur atoms aid in stabilizing the positive charge on the Trp191 radical (*13*).

Since these studies have shown that it is possible to electrostatically destabilize the Trp191 cation radical in CcP, then it also should be possible to carry out the reverse engineering experiment to stabilize the Trp179 cation radical in APX. The first attempt to achieve this goal was to remove the K^+ binding site in APX (*14*). Unfortunately, it appears that K^+ plays an important structural role. The APX mutant lacking K^+ exhibits a large change in the active site, leading to coordination of the catalytic distal His residue to the heme iron, which generates a bis-His complex. The next attempt to achieve this goal, which is the focus of the study presented here, is to introduce the proximal Met residues into APX. The mutant containing all three Met residues has been designated APX3M. A preliminary analysis of APX3M led to the creation of two further mutants building on the APX3M background. First, Trp179 was replaced with Phe in APX3M, producing APX3M/W179F for examining the nature of the compound I radical in APX3M.

The second mutant built on the APX3M background is based on a theoretical study indicating that the heme propionates play a role in stabilization of porphyrin π-cation radicals. Using density functional theory, Guallar et al. (*15*) suggest that shielding of the propionate groups by hydrogen bonding to nearby residues is responsible for stabilization of a porphyrin π-cation radical. Most of the members of the plant, fungal, and bacterial superfamily of heme peroxidases which form a porphyrin π-radical in compound I have an Arg or a Lys residue within H-bonding distance of one of the heme propionates (*3*, *16*−*18*). In APX, Arg172 serves this role. We therefore replaced Arg172 with Asn on the APX3M background to give APX3M/R172N which, according to Guallar et al. (*15*), should further destabilize the porphyrin π-cation radical. In this study, we present steady- and transient-state kinetics and EPR analyses of the various APX mutants designed to increase the stability of a Trp179 cation radical and decrease the stability of the porphyrin π-cation radical in APX compound I.

MATERIALS AND METHODS

Enzymes and reagents for site-directed mutagenesis were purchased from New England Biolabs Inc. (Beverly, MA), Invitrogen Corp. (Carlsbad, CA), and Qiagen Inc. (Valencia,

CA). Chromatography columns were purchased from Qiagen Inc. and Whatman Inc. (Clifton, NJ). Hydrogen peroxide (30%, w/w) was purchased from Sigma. Pyrogallol, sodium ascorbate, potassium ferrocyanide, and guaiacol were purchased from Aldrich or EM Science. All other chemicals were molecular biology grade or better and were purchased from EM Science (Gibbstown, NJ).

Site-Directed Mutagenesis. Oligonucleotide mutagenesis was performed on a pTrc99A vector containing APX with an N-terminal His tag (*14*). Mutagenesis was carried out using the QuickChange site-directed mutagenesis kit from Stratagene in a Perkin-Elmer Gene Amp PCR System 2400 machine. The complementary primers required by this method were obtained from Operon Technologies (Alameda, CA) and were designed as 21−35-mers. The Ser160Met mutation was built onto the wild-type APX gene using the 31-mer 5′-ggacattgttgctctaatgggtggtcacacc and its reverse complement, and this mutant was called APX1M. The PCR products were cut with DpnI to remove the methylated template strands, and this mixture was transformed into the XL1-Blue *Escherichia coli* strain. Once the mutant sequence of APX1M was confirmed by DNA sequencing, the Leu203Met and Gln204Met mutations were built onto the APX1M gene using the 33-mer 5′-ggatggccttatgatgttgccaagtgataaggc-3′ and its reverse complement, using the same mutagenesis method. This mutant was called APX3M. The proximal Trp179 was replaced with Phe in an effort to examine the nature of the radical in the APX3M mutant. This mutation was built onto the APX3M gene using the 21-mer 5′-gggaccattcacttctaatcc and its reverse complement, making the mutant APX3M/W179F. To address the role the propionates play in stabilizing the porphyrin radical in compound I of APX, the Arg172Asn mutation was built onto the APX3M gene using the 25-mer 5′-ctcacaaggagaattctggatttg and its reverse complement. This mutant was called APX3M/R172N. The sequences of all mutants were confirmed by DNA sequencing at the University of California Davis's DBS sequencing facility.

Expression and Purification. Mutant plasmids were transformed into *E. coli* TOPP2 cells, and a single colony was selected for expression. The pTrc99A transformants were grown in Luria broth supplemented with 0.2−0.5% dextrose and 100 μg/mL ampicillin. The bacteria were grown to an optical density of 0.6 at 600 nm before protein expression was induced with 300 μM IPTG. Upon induction, the temperature was reduced to 26 °C, the shaking intensity was reduced to 100 rpm, and the cells were incubated for 12−16 h before they were harvested by centrifugation. Protein was purified according to the method of Cheek et al. (*14*). Briefly, cells were resuspended in 1 column volume of column buffer [50 mM $NaPO_4$ (pH 7.0), 1.4 mM β-mercaptoethanol, 200 mM NaCl, 10 mM imidazole, and 5% glycerol], flash-frozen in liquid N_2, and quickly thawed in 2 volumes of room-temperature column buffer. This solution was kept at 4 °C while PMSF was added to a final concentration of 1 mM and EDTA was added to a final concentration of 0.5 mM. Cells were lysed by the addition of lysozyme to a final concentration of 5 mg/mL followed by incubation on ice for 1 h. This mixture was brought to 20 mM $MgCl_2$ and 5 μg/mL DNase I. After incubation on ice for an additional 1 h, the mixture was centrifuged at 27000*g* for 20 min and the resulting supernatant was loaded onto a 20 mL Ni−NTA column. The column was washed with at least 10 column volumes of column buffer containing 25 mM imidazole. Pure APX was eluted with column buffer containing 200 mM imidazole and dialyzed against 20 mM potassium phosphate buffer (pH 7.4). The protein then was reconstituted with a 5-fold excess of free hemin over the course of 1 h, and after a short centrifugation, the supernatant was loaded onto a DEAE column for removal of the excess heme. Holo-APX was eluted with 100 mM potassium phosphate buffer (pH 7.0), and pure fractions were pooled and dialyzed against 50 mM potassium phosphate buffer (pH 7.0). Purity was examined spectrophotometrically, and protein with an R_z above 1.9 was judged to be pure. Purity was confirmed by SDS−PAGE. The concentration of the dimer was calculated using the extinction coefficient at 403 nm of 114 mM^{-1} cm^{-1}.

Steady-State Activity Assays. The steady-state activity assays of wild-type APX and the mutants APX1M, APX3M, APX3M/W179F, and APX3M/R172N were carried out using ascorbate, guaiacol, pyrogallol, and potassium ferrocyanide using previously published protocols (*19*). All assays were performed at room temperature on a Cary 3E UV−vis spectrophotometer using 50 nM APX monomer and 90 μM H_2O_2 in 50 mM potassium phosphate (pH 7.0) with 0.1 mM EDTA. Ascorbate peroxidase assays were performed using between 10 and 800 μM sodium ascorbate. The oxidation of ascorbate was monitored at 290 nm using an ϵ_{290} of 2.8 mM^{-1} cm^{-1} as the extinction coefficient for oxidized ascorbate. Guaiacol peroxidase activity was measured using between 2.5 and 25 mM guaiacol from a stock of guaiacol in 30% (v/v) ethanol in water and was monitored at 470 nm using an ϵ_{470} of 26.6 mM^{-1} cm^{-1} as the extinction coefficient for oxidized guaiacol. Pyrogallol peroxidase activity was measured using between 75 μM and 4 mM pyrogallol, and absorption was monitored at 430 nm using an extinction coefficient ϵ_{430} of 2.47 mM^{-1} cm^{-1} for oxidized pyrogallol. Finally, activity against potassium ferrocyanide was measured using between 10 and 400 μM potassium ferrocyanide and monitored at 420 nm using an extinction coefficient of oxidation ϵ_{420} of 1 mM^{-1} cm^{-1}. The activity at each substrate concentration was calculated by dividing the change in absorbance by the extinction coefficient. The k_{cat} value was then determined by dividing the units of activity by the millimolar concentration of monomer used in the assay and converting the time scale into seconds.

Transient-State Kinetic Studies. Rates of formation and decay of compound I were determined using an Applied Photophysics Ltd. SX.18MV-R stopped-flow spectrophotometer at room temperature. APX with a heme concentration of 4 μM was mixed with H_2O_2 at concentrations ranging from 2 to 20 μM. The formation of compound I was examined at 403 nm for 20 ms (*20*). The spontaneous decay of compound I was monitored at 420 nm for wild-type APX, APX1M, and APX3M, while the decay was measured at 430 nm for APX3M/W179F and at 425 nm for APX3M/R172N (*20*). These wavelengths were chosen to ensure a maximal change in absorbance for each mutant and were determined by examining the transient-state reaction with a diode array attached to the SX.18MV-R stopped-flow spectrophotometer. Data were fit to a single-exponential curve using Applied Photophysics SX.18MV-R software or Igor Pro (version 3.14) and were analyzed using Igor Pro (version 3.14).

Table 1: Steady-State Kinetics of Wild-Type APX and APX Mutants Using Four Substrates[a]

	ascorbate		guaiacol		pyrogallol		ferrocyanide	
protein	k_{cat} (s^{-1})	K_M (mM)	k_{cat} (s^{-1})	K_M (mM)	k_{cat} (s^{-1})	K_M (mM)	k_{cat} (s^{-1})	K_M (mM)
wild type	33.1	−	16.9	12.2	65.2	0.45	28.4	−
APX1M	12.2	−	6.7	12.5	8.6	0.63	2.0	−
APX3M	8.36	−	4.9	8.1	11.7	0.65	3.2	−
APX3M/W179F	3.1	−	2.8	11.6	2.8	0.20	0.77	−
APX3M/R172N	0.22	−	4.9	11.2	4.9	0.70	0.75	−

[a] The natural substrate, ascorbate, and ferrocyanide do not obey simple Michaelis−Menten kinetics, so it was not possible to determine K_M values from double-reciprocal plots.

Electron Paramagnetic Resonance Studies. EPR spectra were obtained using previously published experimental protocols (*6*). Briefly, 200 μL of 350 μM protein was mixed with 200 μL of 420 μM H_2O_2, giving a 1.20-fold molar excess of peroxide over the heme, and the mixture was transferred to an EPR tube. Samples were frozen within 25 s of initial mixing in an *n*-hexanes/N_2(l) slurry. Electron paramagnetic resonance spectroscopy was carried out on a Bruker ESP300 EPR spectrometer equipped with an air products LTR3 liquid helium cryostat. Data were collected at 10 K with a microwave frequency of 9.388 GHz, a microwave power of 6.375 mW, a receiver gain of 2.00×10^6 (2.00×10^4 for the APX3M/W179F mutant), a modulation frequency of 100 kHz, a modulation amplitude of 1.00 G, and a field sweep rate of 41.94 G/s. Spin equivalents were quantified by using Cu^{2+}-EDTA as a standard (*21*). The same instrument settings were used for the standard and protein samples. All protein samples were prepared at the same concentration.

RESULTS

Steady-State Kinetic Assays. APX does not exhibit Michaelis−Menten kinetics using ascorbate as the substrate. Therefore, k_{cat} values are taken as the maximum velocity at a saturating ascorbate concentration, and the wild-type rate agrees with previously published work (*19*, *22*, *23*). Both Met mutants, APX1M and APX3M, maintain approximately one-third of wild-type activity (Table 1). However, the Trp179Phe and Arg172Asn mutations built onto the APX3M construct resulted in a decrease in activity to ≈1−10% of wild-type activity. The extremely low activity of the Arg172Asn mutant with ascorbate was expected since Arg172 is involved directly in the binding of ascorbate to the enzyme (*23*).

APX has two distinct binding sites for reducing substrates, one for ascorbate at the γ-heme edge near Arg172 (Figure 1), while neutral phenolic substrates are thought to bind near the exposed δ-heme edge (*19*, *23*−*25*). Therefore, to examine the effect of mutations on the two electron transfer pathways, steady-state turnover of other common small molecule substrates was examined. Both aromatic phenolic substrates exhibit Michaelis−Menten kinetics, thus enabling a comparison of both k_{cat} and K_m. As shown in Table 1, all mutants exhibit 29−40% wild-type activity using guaiacol as the substrate, while with pyrogallol, the activity ranges from 4−18% of wild-type activity. Ferrocyanide also was included as a reducing substrate since this is an anionc substrate and might mimic the natural substrate, ascorbate. As shown in Table 1, all mutants exhibit a very low ferrocyanide peroxidase activity ranging from 2 to 11% of wild-type activity.

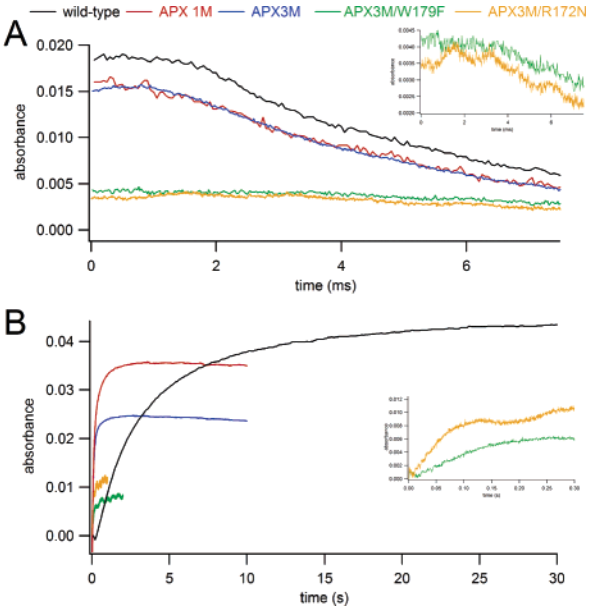

FIGURE 2: Transient-state kinetic traces of compound I formation (A) and its spontaneous decay (B) in wild-type APX, APX1M, APX3M, APX3M/W179F, and APX3M/R172N. Panel A shows the transient-state formation of the porphyrin radical; APX3M/W179F and APX3M/R172N traces are also shown in the inset due to the decrease in the total change in amplitude. Panel B shows the spontaneous decay of the porphyrin radical of compound I; APX3M/W179F and APX3M/R172N traces are again shown in the inset due to the decrease in the total change in amplitude. The data were analyzed and the figures created using Igor Pro (version 3.14).

Table 2: Transient-State Kinetics of Wild-Type APX and APX Mutants[a]

protein	rate of compound I formation ($\times 10^7$ M^{-1} s^{-1})	% wild-type ΔOD	rate of compound I decay (s^{-1})
wild type	3.8	100	0.23
APX1M	1.9	89.1	3.8
APX3M	2.8	82.2	8.3
APX3M/W179F	2.1	21.5	6.0
APX3M/R172N	1.6	23.2	9.2

[a] The % wild-type ΔOD change represents the maximum change in optical density at 403 nm used for measuring compound I formation and is given as the percentage of the wild-type value.

Transient-State Kinetic Studies. Experiments examining the transient-state kinetics of compound I formation and spontaneous decay were carried out to determine the effect of introduction of three Met residues into the proximal pocket on the formation and stability of the porphyrin radical in compound I. Figure 2 shows the stopped-flow traces, and Table 2 provides the rate constants obtained from these data. The second-order rate constants for compound I formation in the mutants are all within a factor of 2 of the wild-type rate (Table 2). The relatively minor reduction in the second-order rate constant for the formation of compound I indicates that the introduction of Met residues into the proximal pocket of APX has little effect on the acid−base catalytic machinery required for compound I formation.

Despite the similar rates of compound I formation, an examination of the amplitude of the change in absorbance

upon mixing APX with H_2O_2 illustrates dramatic differences (Figure 2). While the Met mutants APX1M and APX3M exhibit essentially the same amplitude change in absorbance as wild-type APX for the formation of compound I, the additional Trp179Phe or Arg172Asn mutations yield a reduction in the amplitude of this change at 403 nm (Figure 2). The decrease in absorbance at 403 nm in the APX3M/W179F and APX3M/R172N mutants is less than one-fourth of the magnitude of the wild-type decrease. These results indicate that APX3M/W179F and APX3M/R172N may be unable to form a full equivalent of porphyrin π-cation radical. In addition, all of the mutations decrease the stability of the porphyrin π-cation radical since the rate of decay of compound I in the mutants increases (Figure 2 and Table 2). The spontaneous decay of compound I occurs 16−40 times more rapidly in the mutants than in the wild type (Table 2). These experiments do not allow any firm conclusions about whether a full oxidizing equivalent resides on the porphyrin to be made since the rapid formation and decay could lead to a mixture of states. Nevertheless, these results do show that the stability of the porphyrin π-cation and most likely the total amount of porphyrin radical formed are decreased in the mutants.

Electron Paramagnetic Resonance. EPR spectra of wild-type APX, APX1M, APX3M, APX3M/W179F, and APX3M/R172N were collected approximately 25 s after the addition of H_2O_2. Figure 3 shows the EPR spectra for wild-type APX, APX3M, and APX3M/W179F together with the spin equivalents estimated by comparison to a Cu^{2+}-EDTA standard. Previously recorded EPR spectra for aged compound I, sometimes called APX I*, showed a small $g_{||} = 2.038$ and $g_{\perp} = 2.004$ feature which was shown to be a Trp radical, most likely Trp179 (*6*, *26*−*28*). The spectra of wild-type APX and APX3M show a similar $g_{||} = 2.037$ and $g_{\perp} = 2.006$ signal. The intensity of the signal in APX3M is much larger and more cleanly resolved than the signal seen in wild-type APX compound I*. In addition, the total number of spin equivalents increases from 0.09 in the wild type to 0.24 in APX3M. Therefore, the Met residues introduced into the proximal pocket of APX promote formation of the Trp179 radical. If the APX3M radical is a Trp radical, then the APX3M/W179F mutant should exhibit quite different EPR properties. This mutant shows a much larger isotropic $g = 2.006$ signal (0.78 spin equivalent) and lacks the $g = 2.037$ peak indicating that, as expected, APX3M/W179F compound I* no longer forms a Trp radical. The EPR spectrum of APX3M/W179F is most likely that of a Tyr radical since the spectrum closely resembles that of the CcP compound I mutant, lacking the proximal Trp residue, where the radical is known to reside on a Tyr (*29*). The EPR spectra of APX1M and APX3M/R172N resemble that of APX3M (data not shown).

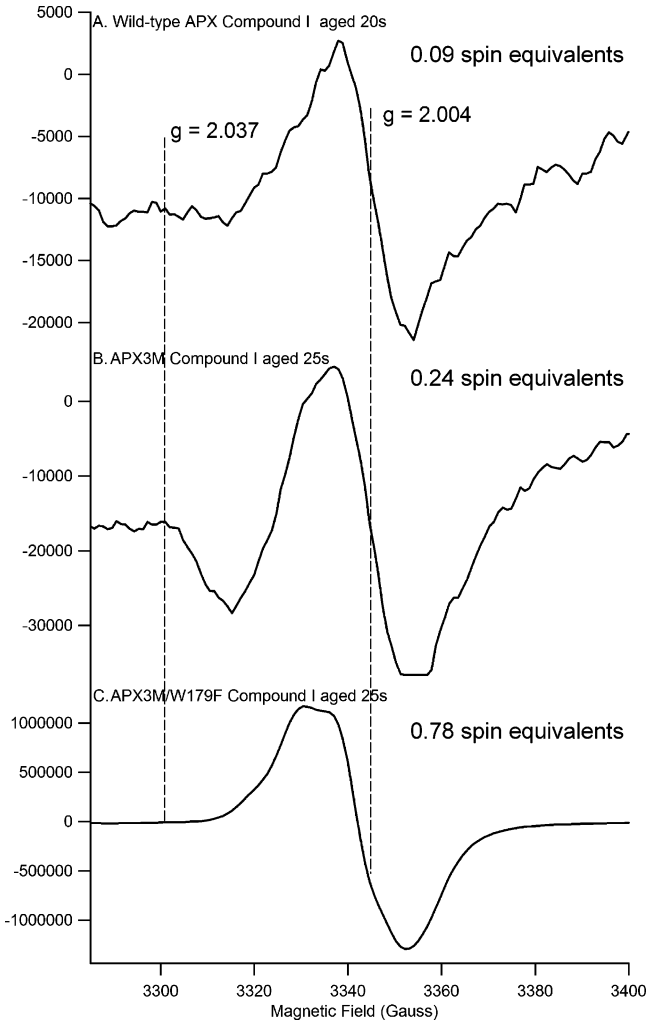

FIGURE 3: Electron paramagnetic resonance spectra of the compound I species of wild-type APX (A) and mutants APX3M (B) and APX3M/W179F (C) were collected on samples frozen approximately 50 s after the initial formation of compound I. The data in panels A−C have been scaled so that relative intensities are directly comparable. The addition of Met residues into the proximal side of APX results in the $g = 2.004$ signal increasing in size and becoming more symmetrical. An additional $g = 2.037$ signal also appears in APX3M which is indicative of a Trp radical; this signal disappears when the proximal Trp residue is mutated to Phe. The spectrum of APX3M/W179F appears to be more like that of an isolated Tyr radical. The total number of spin equivalents relative to the Cu^{2+}-EDTA standard is also given.

DISCUSSION

Our current work coupled with previous work on CcP illustrates that it is possible to control the location of radical sites in peroxidases by engineering in the appropriate electrostatic environment. Previous work with CcP has shown that the proximal Met residues, M172, M230, and M231 (CcP numbering), play an important role in the electrostatic stabilization of the Trp radical in CcP (*13*). When these residues are replaced with the corresponding residues in APX in the presence of an engineered potassium binding site, the wild-type CcP EPR signature is replaced with a Tyr signal. Studies of the lifetime of the Trp radical, as examined by transient-state kinetics of a single-turnover reaction with ferrous cytochrome *c*, show that the half-life of this radical is reduced to less than 25 ms when all of the Met residues are removed from the proximal pocket. The study presented here provides support to these previous findings by showing that the introduction of three Met residues into homologous positions in the proximal pocket of APX results in substantial destabilization of the compound I porphyrin radical and the total amount of porphyrin radical formed. Most significantly, the EPR data exhibit a more prominent Trp radical signal. The $g_{||} = 2.038$ signal (Figure 3) has been shown to be associated with a Trp radical in APX after compound I is allowed to age (*26*). The $g_{||} = 2.038$ signal also appears in

a mutant of horseradish peroxidase compound I when the proximal side Phe221 is replaced with Trp (*27*). Phe221 in horseradish peroxidase is the homologue to Trp191 in CcP and Trp179 in APX. Since APX has only two Trp residues, Trp179 in the proximal pocket and Trp41 in the distal pocket, it is very likely that Trp179 is the site of radical formation in the APX3M mutants. That the APX3M/W179F mutant lacks the $g_{||} = 2.038$ peak further supports Trp179 as the site of radical formation. Interestingly, the APX3M/W179F EPR spectrum (Figure 3) closely matches that of CcP which lacks the proximal Trp, where it is known that the radical resides on a Tyr residue, most likely Tyr236 (*29*). There are seven Tyr residues in APX, and three of these, Tyr190, Tyr224, and Tyr235, are within 20 Å of the heme iron. The most likely candidate of these three residues is Tyr190 which is located only 7.6 Å from the heme plane.

Most of our work on CcP and APX has centered on how to stabilize or destabilize a Trp radical. However, most peroxidases form a porphyrin radical so it also is important to address the question of how the protein environment helps to stabilize a porphyrin radical in most heme peroxidases (*15*, *30*). Density functional theory has provided an interesting explanation (*15*, *31*). The heme propionates are able to transfer electron density to the porphyrin radical, thus diminishing the degree of porphyrin π-cation radical character. However, salt bridging to the heme propionates negates this effect, thus resulting in a more stable porphyrin π-cation radical. Although this study focused on cytochrome P450, it is interesting to note that most heme peroxidases that form porphyrin π-cation radicals have at least one Arg or Lys residue H-bonding or forming a salt bridge, respectively, with the heme propionates. CcP which does not form a detectable porphyrin radical also does not have an Arg or Lys residue H-bonding or forming a salt bridge, respectively, with at least one propionate group. It was these observations that prompted us to generate the APX3M/R172N mutant since Arg172 in APX directly interacts with one heme propionate. This mutant forms the least stable porphyrin radical, thus supporting the view that salt bridges or H-bonding to the heme propionates promotes porphyrin π-cation radical formation.

The mutations also affect the overall function of the enzyme as seen by the reduction in activity in all of the mutant constructs. In steady-state assays with the small molecule substrates ascorbate, guaiacol, pyrogallol, and potassium ferrocyanide, the oxidation of the substrate by the mutant enzymes occurred more slowly than in experiments carried out using the wild-type enzyme (Table 1). It is generally thought that neutral aromatic substrates such as guaiacol and pyrogallol react at the δ-heme edge [Figure 1 (*23*)] which would enable close interaction with the porphyrin radical. Since the mutants exhibit a decrease in the stability of the porphyrin π-cation radical and the amount formed, it is not surprising that the mutants exhibit a decreased rate of steady-state turnover.

ACKNOWLEDGMENT

We thank Joumana Jamal and Dr. David Mandelman for helpful discussions of steady-state assays. We also thank Dr. Patrick Farmer for helpful discussions of EPR data collection and analysis and Drs. Marcus Ribbe and Michael Goldfeld for EPR data collection.

NOTE ADDED AFTER ASAP PUBLICATION

This paper was published ASAP 10/04/05. The name of the mutant in the final row of Tables 1 and 2 has been corrected; the corrected version was published 10/06/05.

REFERENCES

1. Sivaraja, M., Goodin, D. B., Smith, M., and Hoffman, B. M. (1989) Identification by ENDOR of Trp191 as the free-radical site in cytochrome *c* peroxidase compound ES, *Science 245*, 738−740.
2. Jensen, G. M., Bunte, S. W., Warshel, A., and Goodin, D. B. (1998) Energetics of cation radical formation at the proximal active site tryptophan of cytochrome *c* peroxidase and ascorbate peroxidase, *J. Phys. Chem. B 102*, 8221−8228.
3. Patterson, W. R., and Poulos, T. L. (1994) Characterization and crystallization of recombinant pea cytosolic ascorbate peroxidase, *J. Biol. Chem. 269*, 17020−17024.
4. Pappa, H., Patterson, W. H., and Poulos, T. L. (1996) The homologous tryptophan critical for cytochrome *c* peroxidase function is not essential for ascorbate peroxidase activity, *J. Biol. Inorg. Chem. 1*, 66.
5. Patterson, W. R., and Poulos, T. L. (1995) Crystal structure of recombinant pea cytosolic ascorbate peroxidase, *Biochemistry 34*, 4331−4341.
6. Patterson, W. R., Poulos, T. L., and Goodin, D. B. (1995) Identification of a porphyrin π-cation radical in ascorbate peroxidase compound I, *Biochemistry 34*, 4342−4345.
7. Mittler, R., and Zilinskas, B. A. (1991) Purification and characterization of pea cytosolic ascorbate peroxidase, *Plant Physiol. 97*, 962−968.
8. Mittler, R., and Zilinskas, B. A. (1991) Molecular cloning and nucleotide sequence analysis of a cDNA encoding pea cytostolic ascorbate peroxidase, *FEBS Lett. 289*, 257−259.
9. Bonagura, C. A., Sundaramoorthy, M., Bhaskar, B., and Poulos, T. L. (1999) The effects of an engineered cation site on the structure, activity, and EPR properties of cytochrome *c* peroxidase, *Biochemistry 38*, 5528−5545.
10. Bonagura, C. A., Sundaramoorthy, M., Pappa, H. S., Patterson, W. R., and Poulos, T. L. (1996) An engineered cation site in cytochrome *c* peroxidase alters the reactivity of the redox active tryptophan, *Biochemistry 35*, 6107−6115.
11. Bhaskar, B., Bonagura, C. A., Li, H., and Poulos, T. L. (2002) Cation-induced stabilization of the engineered cation-binding loop in cytochrome *c* peroxidase (CcP), *Biochemistry 41*, 2684−2693.
12. Poulos, T. L., Barrows, T., Bhaskar, B., Bonagoura, C. A., and Li, H. (2001) Coupling crystallography and computational biochemistry in understanding heme enzyme structure and function, *Int. J. Quantum Chem. 88*, 211−219.
13. Barrows, T. P., Bhaskar, B., and Poulos, T. L. (2004) Electrostatic control of the tryptophan radical in cytochrome *c* peroxidase, *Biochemistry 43*, 8826−8834.
14. Cheek, J., Mandelman, D., Poulos, T. L., and Dawson, J. H. (1999) A study of the K^+ site mutant of ascorbate peroxidase. Mutations of protein residues on the proximal side of the heme cause changes in the iron ligation on the distal side, *J. Biol. Inorg. Chem. 4*, 64−72.
15. Guallar, V., Baik, M. H., Lippard, S. J., and Friesner, R. A. (2003) Peripheral heme substituents control the hydrogen-atom abstraction chemistry in cytochromes P450, *Proc. Natl. Acad. Sci. U.S.A. 100*, 6998−7002.
16. Sundaramoorthy, M., Kishi, K., Gold, M. H., and Poulos, T. L. (1994) The crystal structure of manganese peroxidase from *Phanerochaete chrysosporium* at 2.06 Å resolution, *J. Biol. Chem. 269*, 32759−32767.
17. Poulos, T. L., Edwards, S. L., Wariishi, H., and Gold, M. H. (1993) Crystallographic refinement of lignin peroxidase at 2 Å, *J. Biol. Chem. 268*, 4429−4440.
18. Gajhede, M., Schuller, D. J., Henriksen, A., Smith, A. T., and Poulos, T. L. (1997) Crystal structure of horseradish peroxidase C at 2.15 Å resolution, *Nat. Struct. Biol. 4*, 1032−1038.
19. Mandelman, D., Jamal, J., and Poulos, T. L. (1998) Identification of two electron-transfer sites in ascorbate peroxidase using chemical modification, enzyme kinetics, and crystallography, *Biochemistry 37*, 17610−17617.
20. Marquez, L. A., Quitoriano, M., Zilinskas, B. A., and Dunford, H. B. (1996) Kinetic and spectral properties of pea cytosolic ascorbate peroxidase, *FEBS Lett. 389*, 153−156.

21. Svistunenko, D. A., Sharpe, M. A., Nicholls, P., Wilson, M. T., and Cooper, C. E. (2000) A new method for quantitation of spin concentration by EPR spectroscopy: Application to methemoglobin and metmyoglobin, *J. Magn. Reson. 142*, 266−275.
22. Mandelman, D., Schwarz, F. P., Li, H., and Poulos, T. L. (1998) The role of quaternary interactions on the stability and activity of ascorbate peroxidase, *Protein Sci. 7*, 2089−2098.
23. Bursey, E. H., and Poulos, T. L. (2000) Two substrate binding sites in ascorbate peroxidase: The role of arginine 172, *Biochemistry 39*, 7374−7379.
24. Sharp, K. H., Mewies, M., Moody, P. C., and Raven, E. L. (2003) Crystal structure of the ascorbate peroxidase-ascorbate complex, *Nat. Struct. Biol. 10*, 303−307.
25. Sharp, K. H., Moody, P. C. E., Brown, K. A., and Raven, E. L. (2004) Crystal Strucutre of the Ascorbate Peroxidase−Salicylhyroxamic Acid Complex, *Biochemistry 43*, 8644−8651.
26. Hiner, A. N., Martinez, J. I., Arnao, M. B., Acosta, M., Turner, D. D., Lloyd Raven, E., and Rodriguez-Lopez, J. N. (2001) Detection of a tryptophan radical in the reaction of ascorbate peroxidase with hydrogen peroxide, *Eur. J. Biochem. 268*, 3091−3098.
27. Morimoto, A., Tanaka, M., Takahashi, S., Ishimori, K., Hori, H., and Morishima, I. (1998) Detection of a tryptophan radical as an intermediate species in the reaction of horseradish peroxidase mutant (Phe-221 → Trp) and hydrogen peroxide, *J. Biol. Chem. 273*, 14753−14760.
28. Sahlin, M., Cho, K. B., Potsch, S., Lytton, S. D., Huque, Y., Gunther, M. R., Sjoberg, B. M., Mason, R. P., and Graslund, A. (2002) Peroxyl adduct radicals formed in the iron/oxygen reconstitution reaction of mutant ribonucleotide reductase R2 proteins from *Escherichia coli*, *J. Biol. Inorg. Chem. 7*, 74−82.
29. Musah, R. A., and Goodin, D. B. (1997) Introduction of novel substrate oxidation into cytochrome *c* peroxidase by cavity complementation: Oxidation of 2-aminothiazole and covalent modification of the enzyme, *Biochemistry 36*, 11665−11674.
30. Asakura, T., and Yonetani, T. (1969) Studies on cytochrome *c* peroxidase. XIV. Recombination of apoenzyme with protoheme dialkyl esters and etioheme, *J. Biol. Chem. 244*, 4573−4579.
31. de Visser, S. P., Shaik, S., Sharma, P. K., Kumar, D., and Thiel, W. (2003) Active species of horseradish peroxidase (HRP) and cytochrome P450: Two electronic chameleons, *J. Am. Chem. Soc. 125*, 15779−15788.
32. Pettersen, E. F., Goddard, T. D., Huang, C. C., Couch, G. S., Greenblatt, D. M., Meng, E. C., and Ferrin, T. E. (2004) UCSF Chimera: A visualization system for exploratory research and analysis, *J. Comput. Chem. 25*, 1605−1612.
33. Collaborative Computational Project, No. 4 (1994) The CCP4 Suite: Programs for Protein Crystallography, *Acta Crystallogr. D50*, 760−763.

BI0507128